

Photoluminescence and thermoluminescence properties of SnO₂ nanoparticles embedded in Li₂O-K₂O-B₂O₃ with Cu-doping

Haydar Aboud^{1,2*}, H. Wagiran¹, R. Hussin¹, Saad Saber¹, and M. A. Saeed¹

¹Department of Physics, Faculty of Science, Universiti Teknologi Malaysia, 81310, Skudai, Johor, Malaysia

²Baghdad College of Economic Sciences University, Iraq

*Corresponding author: han55608@yahoo.com

Received April 3, 2013; accepted July 9, 2013; posted online September 3, 2013

Cu-doped borate glass co-doped with SnO₂ nanoparticles is fabricated by melt quenching. The structure and morphology of the samples are examined by X-ray diffraction and field emission scanning electron microscopy. Up-conversion enhancement is observed in the photoluminescence (PL) and thermoluminescence (TL) intensities of the glass. PL emission spectra are identified in the blue and green regions, and a fourfold increase in emission intensity may be observed in the presence of embedded SnO₂ nanoparticles. The glow curve is recorded at 215 °C, and fourfold increases in TL intensity are obtained by addition of 0.1 mol% SnO₂ nanoparticles to the glass. Higher TL responses of the samples are observed in the energy range of 15–100 KeV. At energy levels greater than ~0.1 MeV, however, flat responses are obtained. The activation energy and frequency factor of the second-order kinetic reaction are calculated by the peak shape method.

OCIS codes: 160.2750, 160.4236, 160.5690, 260.3800.

doi: 10.3788/COL201311.091603.

Borate glass is a favorable host for different metals (e.g., transition and rare earth metals) and an interesting material for application in strong nonlinear optics, quantum electronics, and large electronic band gaps because of its lattice, chemical, and environmental stability, as well as mechanical robustness^[1–3]. Borates are attractive candidates as host lattices in thermoluminescence dosimetry (TLD)^[4–6]. In recent years, borate glass has become the subject of intensive investigations because of its technological and scientific importance. It is a promising material for many applications because of its high sensitivity, very low cost, easy handling, and facile preparation^[7,8].

Magnesium tetraborate, barium betaborate, and lithium tetraborate are three borates commonly used in TLD^[9]. Lithium triborate (LiB₃O₅) has recently received significant research attention because of its TL properties. The effective atomic numbers of lithium triborate and lithium tetraborate are very close to that of biological tissue, which indicates that these compounds are more significant than others for medical and personnel dosimetry usage^[10]. Many studies have been conducted to investigate the TL properties of borates, such as Li₂B₄O₇:Cu^[11], Li₂B₄O₇:Cu,In,Ag^[12], Li₂B₄O₇:Cu,Ag,P^[13], Li₂B₄O₇:Mn^[14], Li₂B₄O₇:Mn,Si^[15], and Li₂K₂B₂O₃:CuO, MgO^[16]. In this letter, the photoluminescence (PL) and TL properties of borates, including dose response, glow curve, energy response, and kinetic parameters, are determined and explored in detail.

Powder samples composed of 20Li₂O-10K₂O-(70-x)B₂O₃-xCu, where x=0, 0.05, 0.1, 0.25, 0.5, 0.75, and 1.0 mol%, and 20Li₂O-10K₂O-(69.9-y)B₂O₃-0.1Cu-ySnO₂, where y=0.05%, 0.1%, and 0.5%, were prepared (see Table 1) by melt quenching. SnO₂ nanoparticles were

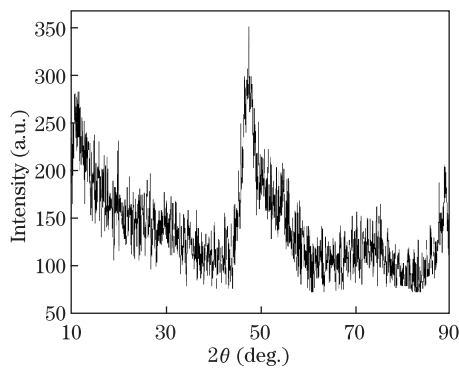
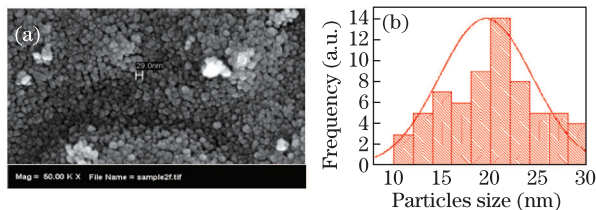
synthesized by the sol-gel method^[17]. The batch mixture (15 g) was prepared using raw material powder (99.99%-purity, Sigma-Aldrich, Germany). The powder was placed in a porcelain crucible and mechanically mixed with each sample for approximately 30 min to obtain a homogeneous mixture. The mixtures were melted in a platinum crucible in an electric furnace set to 1100 °C for 30 to 60 min, depending on the time required for the resultant product to become clear and homogeneous. When the required viscosity had been achieved, the samples were quenched in steel plates, annealed at 400 °C for 3 h, and then cooled to room temperature. The structure of the samples was analyzed by X-ray diffraction (XRD) to confirm their amorphous nature. Morphological analysis of the samples was performed by field emission scanning electron microscopy (FE-SEM). Optical absorption spectra were examined at room temperature using a Shimadzu 3101 ultra-violet-visible-near-infrared (UV-Vis-NIR) spectrophotometer in the range of 200–2000 nm. PL spectra were obtained using a Perkin Elmer LS55 luminescence spectrophotometer. The linear accelerator Primus (LINAC Primus) at the Department of Radiotherapy and Oncology, Hospital Sultan Ismail, Johor Bahru, Malaysia, was used to irradiate the samples with photons of very high energy at different dose rates. A TLD-Reader 4500 from Harshaw Company was used to measure TL at the Malaysian Nuclear Agency.

The XRD pattern of a borate glass sample doped with SnO₂ nanoparticles is shown in Fig. 1. The pattern reveals that the glass is completely amorphous because of the presence of diffuse peaks and the absence of sharp Bragg peaks. Several sharp peaks appear in the current host, and their presence may be attributed to overlapping peaks. Sn species, particularly Sn⁴⁺, is abundant in the prepared host samples. The reactivity of Sn with other

Table 1. Nominal Composition of $\text{Li}_2\text{O-K}_2\text{O-B}_2\text{O}_3$ Co-doped with Cu and SnO_2 Nanoparticles

Sample No.	Composition (mol%)				
	B_2O_3	Li_2O	K_2O	Cu	SnO_2
S0	70.00	20	10	0.00	0.00
S1	69.95	20	10	0.05	0.00
S2	69.90	20	10	0.10	0.00
S3	69.75	20	10	0.25	0.00
S4	69.50	20	10	0.50	0.00

Sample No.	Composition (mol%)				
	H_3BO_3	Li_2CO_3	K_2CO_3	Cu	SnO_2
S5	69.85	20	10	0.1	0.05
S6	69.80	20	10	0.1	0.10
S7	69.70	20	10	0.1	0.20

Fig. 1. XRD pattern obtained for borate glass co-doped with 0.1% SnO_2 nanoparticles.Fig. 2. (a) (Color online) FE-SEM image of a borate glass sample co-doped with 0.1% SnO_2 nanoparticles. (b) Particle size distribution histogram of the sample in (a).

oxides is enhanced, resulting in precipitation and formation of crystalline bonds. FE-SEM images of a borate glass sample are presented to examine the microstructures of the SnO_2 nanoparticles. Figure 2(a) shows a cross-sectional FE-SEM image of the glass sample. The wide distribution of nanoparticles may be observed in the glass. Figure 2(b) shows that the average size of the SnO_2 nanoparticles is approximately 21 nm.

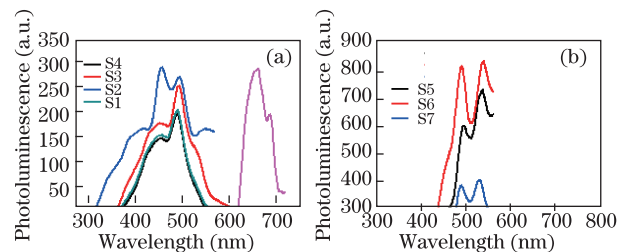
PL emission spectra of borate glass samples with and without SnO_2 nanoparticles were obtained at an excitation wavelength of 650 nm. The emission spectra (Fig. 3(a)) indicate two obvious peaks and a broad band within the blue emission range at 450 and 490 nm. Peak intensities progressively increase with increasing Cu concentration from 0.05% to 0.1%. The up-conversion emission peak is attributed to transitions of $3d^9 4s^1 \rightarrow 3d^{10}$ and $3d^9$ [18,19]. The sequential absorption of two or more photons leads to enhancement of the localized electric

field and emission of light at wavelengths shorter than the excitation wavelength. However, intensity saturation and quenching are obtained when the Cu concentration is increased to over 0.1% and is especially pronounced at 0.5% Cu.

The influence of SnO_2 nanoparticles on PL intensity is illustrated in Fig. 3(b). Enhanced PL intensity is observed when the nanoparticles are introduced to the host matrix. Increasing the concentration of SnO_2 nanoparticles from approximately 0% to 0.1% results in a threefold nonlinear enhancement in emission. This enhancement may be due to energy transfer from the surface of the nanoparticles to the emitter ions, energy transfer from the ions to the nanoparticles, and or the enhanced localized electric field. The emission spectra shift from blue to green, which is due to a very common defect in glass, i.e., oxygen vacancies. Luminescence quenching is observed with increasing SnO_2 nanoparticle concentration up to 0.5%, which is attributed to an increase in the agglomeration of nanoparticles. Decreases in the surface-to-volume ratio and energy transfer from Cu to the surface of SnO_2 nanoparticles are also observed.

The luminescence intensity is a result of radiative recombinations between electrons, which are released from the electron center upon heating and an antibonding molecular orbital of the nearest oxygen hole center. TL emission in the borate glasses is usually possible only at low temperatures because of this recombination process[20]. During heating, electrons confined in metal ions are released and become trapped by holes in recombination centers, resulting in the production of TL light[21]. Figure 4 shows the glow curves of glass samples with different SnO_2 concentrations after photon irradiation with 1 Gy at 6 MV. After 24 h of irradiation, the glow curve was recorded at 20 °C/s and annealing temperature of 400 °C. The maximum TL peak of the samples appears at 215 °C, and the highest TL response is observed in glass with 0.1-mol% SnO_2 . A nearly four-fold increase in TL intensity is obtained when 0.1-mol% Cu-doped lithium potassium borate is co-doped with 0.1-mol% SnO_2 . Such behavior is attributed to the creation of new traps and recombination centers when SnO_2 nanoparticles are added to the Cu-doped sample.

A TLD detector exhibits a linear relationship between TL intensity and absorbed dose. The light emitted by a TLD material represents the sum of contributions of different peaks, resulting in a linear dose characteristic[22]. The samples were exposed to 6-MV

Fig. 3. (Color online) Photoluminescence spectra of borate glass. (a) Emission spectra of Cu-doped borate glass co-doped with different concentrations of SnO_2 nanoparticles. (b) Emission spectra of 0.1-mol% Cu-doped glass co-doped with different concentrations of SnO_2 nanoparticles upon excitation at 650 nm.

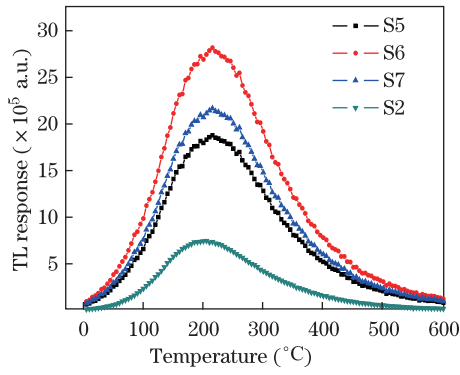


Fig. 4. (Color online) Glow curve of irradiated 0.1-mol% Cu-doped lithium potassium borate co-doped with 0.1-mol% SnO₂ nanoparticles.

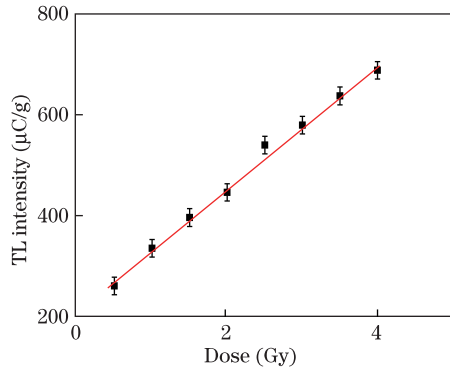


Fig. 5. (Color online) TL responses of 0.1-mol% Cu-doped lithium potassium borate co-doped with 0.1-mol% SnO₂ nanoparticles subjected to 6-MV photon irradiation.

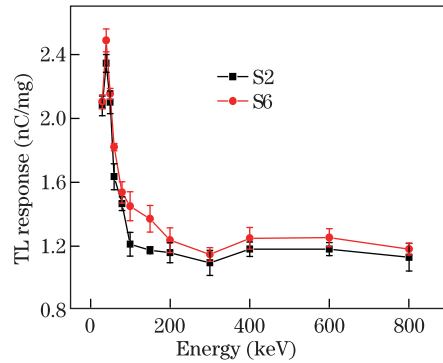


Fig. 6. (Color online) TL responses of Cu-doped samples with and without co-doping with SnO₂ versus photon energies after exposure to an absorbed dose of 0.2 mGy.

photon irradiation with different absorbed doses of 0.5–4.0 Gy. Figure 5 reveals that the TL intensity increases linearly with the photon dose. TL responses increase linearly with increasing dose up to 4.0 Gy.

The TL responses of the borate samples at various photon energies were also determined for low-energy photons (30–800 keV). The TL responses of Cu-doped samples with and without co-doping with SnO₂ were recorded after exposure to an absorbed dose of 0.2 mGy, and the results are shown in Fig. 6. The figure indicates that both samples show a flat response at energy levels greater than ~0.1 MeV, which is the case for all materials with constituent elements having *K*-edges of less than 1 keV.

Higher responses due to the dominance of the photoelectric effect are observed in the energy range of 15–100 keV. The photoelectric component of the mass energy absorption coefficient of a certain element varies approximately as Z^2 . The TL responses of co-doped samples are consistently slightly higher than those of samples doped with only Cu.

One of the main objectives of a TL experiment is to extract data from an experimental glow curve, or a series of glow-curves, and use these data to calculate various parameters associated with the charge transfer process of the material under study. These parameters include the trap depth, E , the frequency factor, s , and the order of the kinetic reaction. The peak shape method was employed to determine the kinetic parameters of the samples. The activation energy is given by

$$E_{\alpha} = C_{\alpha} \left(\frac{kT_M^2}{\alpha} \right) - b_{\alpha} (2kT_M), \quad (1)$$

where α can be either $\tau = T_M - T_1$, $\delta = T_2 - T_M$, or $\omega = T_2 - T_1$. T_M corresponds to the maximum temperature, and T_1 and T_2 respectively represent the half TL intensity temperatures at low and high regions of the peak. T_M , T_1 , and T_2 of glass co-doped with SnO₂ are 215, 136, and 310 °C, respectively, as shown in Fig. 7. The values of C_{α} and b_{α} depend on the parameter selected for analysis^[23]. If γ is used, i.e., α is replaced by γ , then

$$C_{\tau} = 1.510 + 3.0(\mu - 0.42), \quad b_{\tau} = 1.58 + 4.2(\mu - 0.42). \quad (2)$$

On the other hand, if δ is used:

$$C_{\delta} = 0.976 + 7.3(\mu - 0.42), \quad b_{\delta} = 0. \quad (3)$$

If ω is used:

$$C_{\omega} = 2.52 + 10.2(\mu - 0.42), \quad b_{\omega} = 1. \quad (4)$$

The geometric shape factor, $\mu = 0.546$, is very close to the theoretical value for a second-order kinetic reaction, $\mu = 0.52$. τ , δ , and ω are 79, 95, and 174, respectively. Table 2 reveals that the C_{α} and b_{α} depend on τ , δ , or ω . The activation energy for the second-order kinetic reaction was determined using the peak shape method, and results from Eq. (1) are presented in Table 3.

Table 2. Values of C_{α} and b_{α} Depending on τ , δ , or ω for Co-doped SnO₂

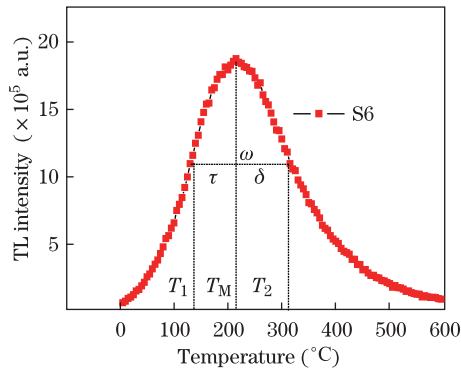
Values	τ	δ	ω
C_{α}	1.88	1.895	3.805
b_{α}	2.109	0	1

Table 3. Activation Energy of Glass Samples Co-doped with SnO₂

Chen's Method			
E_{τ} (eV)	E_{δ} (eV)	E_{ω} (eV)	Mean Value
0.31	0.40	0.35	0.35

Table 4. Trap Frequency Factor of Samples Co-doped with SnO₂

Chen's Method			
S_τ (s ⁻¹)	S_δ (s ⁻¹)	S_ω (s ⁻¹)	Mean Value(s ⁻¹)
1.7×10^4	1.0×10^5	0.26×10^5	2.6×10^4

Fig. 7. (Color online) Geometric parameters of borate glass co-doped SnO₂.

The s for the samples was calculated using

$$s = \beta E K T_M^2 \exp(E/kT_M), \quad (5)$$

where β is the heating rate, E is the activation energy, and T_m is the maximum peak temperature. Results are presented in Table 4.

In conclusion, the properties of Cu-doped borate glass co-doped with SnO₂ nanoparticles are studied. Two obvious peaks and a broad band are identified at 450 and 490 nm. Within the blue luminescence emission range and with the addition of SnO₂ nanoparticles, there is shift to blue and green emission. The PL intensity may be gradually increased by increasing the doping concentration from 0.05 to 0.1 mol%, and quenching was observed at concentrations over 0.1 mol%. A three-fold increase in PL intensity is observed with increasing doping concentration of SnO₂ nanoparticles. TL characterization, including the dose response, energy response, and kinetic parameters, is also investigated. TL measurements reveal high dose responses from 0.5 to 4.0 Gy. The energy responses of borate glass with and without SnO₂ nanoparticles is high from 15 to 100 KeV but flat beyond 0.1 MeV. The activation energy and frequency values obtained by the peak shape method are 0.35 and 2.6×10^4 , respectively.

The authors would like to thank the Ministry of Higher Education for providing the research grant and the Universiti Teknologi Malaysia (UTM) for providing research

assistance. The authors are thankful to RMC, UTM for providing research funding to complete this work.

References

1. Y. Saleh, S. Hashim, W. Saridan, W. Hassan, and A. Ramli, *J. Mol. Struct.* **1026**, 159 (2012).
2. M. Elkholy, *J. Lumin.* **130**, 1880 (2010).
3. A. El-Adawy, N. Khaled, A. R. El-Sersy, A. Hussein, and H. Donya, *Appl. Radiat. Isot.* **68**, 1132 (2010).
4. Z. Xiong, P. Ding, Q. Tang, J. Chen, and W. Shi, *Adv. Mat. Res.* **160**, 252 (2011).
5. S. Puppallwar, S. Dhoble, N. Dhoble, and K. Animesh, *Nucl. Instrum. Methods B* **274**, 167 (2012).
6. H. Aboud, H. Wagiran, I. Hossainand, and R. Hussin, *Int. J. Phys. Sci.* **7**, 929 (2012).
7. Y. S. M. Alajerami, S. Hashim, A. T. Ramli, M. A. Saleh, A. B. B. A. Kadir, and M. I. Saripan, *Chin. Phys. Lett.* **30**, 017801 (2013).
8. G. Ramadevudu, S. R. L. Srinivasa, M. S. A. Hameed, and M. C. Narasimha, *Int. J. Eng. Sci. Technol.* **3**, 6998 (2011).
9. Z. T. Yu, Z. Shi, W. Chen, Y. S. Jiang, H. M. Yuan, and J. S. Chen, *J. Chem. Soc., Dalton Trans.* **9**, 2031 (2002).
10. G. V. Rao, P. Y. Reddy, and N. Veeraiah, *Mater. Lett.* **57**, 403 (2002).
11. C. Furetta, M. Prokic, R. Salamon, V. Prokic, and G. Kitis, *Nucl. Instrum. Methods in Phys. Res. A* **456**, 411 (2001).
12. M. Prokic, *Radiat. Meas.* **33**, 393 (2001).
13. N. Can, T. Karali, P. D. Townsend, and F. Yildiz, *J. Phys. D Appl. Phys.* **39**, 2038 (2006).
14. J. H. Schulman, R. D. Kirk, and E. J. West, in *Proceedings of the International Conference on Luminescence Dosimetry CONF-650637* 113 (1967).
15. G. Kitis, C. Furetta, M. Prokic, and V. Prokic, *J. Phys. D: Appl. Phys.* **33**, 1252 (2000).
16. Y. S. M. Alajerami, S. Hashim, A. T. Ramli, M. A. Saleh, and T. Kadni, *Radiat. Prot. Dosimetry* **155**, 1 (2013).
17. M. Aziz, S. Abbas, and W. R. W. Baharom, *Mater. Lett.* **91**, 31 (2013).
18. T. C. Chen and T. G. Stoebe, *Radiat. Prot. Dosimetry* **78**, 101 (1998).
19. Y. S. M. Alajerami, S. Hashim, W. M. S. W. Hassan, and A. T. Ramli, *Phys. B* **407**, 2390 (2012).
20. W. M. Pontuschka, L. S. Kanashiro, and L. C. Courrol, *Phys. Chem. Glass* **27**, 37 (2012).
21. S. M. Del Nery, W. M. Pontuschka, S. Isotani, and C. G. Rouse, *Phys. Rev. B* **49**, 3760 (1994).
22. H. Wagiran, I. Hossain, D. Bradley, A. N. H. Yaakob, and T. Ramli, *Chin. Phys. Lett.* **29**, 027802 (2012).
23. S. W. S. McKeever, M. Moscovitch, and P. D. Townsend, *Thermoluminescence Dosimetry Materials: Properties and Uses* (Nuclear Technology Publishing, Kent, 1995).